International Journal of Remote Sensing
Vol. 27, No. 22, 20 November 2006, 4963–4990

Taylor & Francis
Taylor & Francis Group

Review Article

Fractal analysis of remotely sensed images: A review of methods and applications

W. SUN*†, G. XU‡, P. GONG§ and S. LIANG¶

†Department of Geography and Planning, Grand Valley State University, Allendale, MI 49401, USA. e-mail: sunwa@gvsu.edu

‡Department of Geography and Planning, Grand Valley State University, Allendale, MI 49401, USA. e-mail: xug@gvsu.edu

§Department of Environmental Science, Policy & Management, University of California, Berkeley, 151 Hilgard Hall, CA94720, USA. e-mail: gong@nature.berkeley.edu

¶Department of Geography, University of Maryland, College Park, MD 20742, USA. e-mail: sliang@geog.umd.edu

(*Received 12 June 2005; in final form 8 March 2006*)

Mandelbrot's fractal geometry has sparked considerable interest in the remote sensing community since the publication of his highly influential book in 1977. Fractal models have been used in several image processing and pattern recognition applications such as texture analysis and classification. Applications of fractal geometry in remote sensing rely heavily on estimation of the fractal dimension. The fractal dimension (*D*) is a central construct developed in fractal geometry to describe the geometric complexity of natural phenomena as well as other complex forms. This paper provides a survey of several commonly used methods for estimating the fractal dimension and their applications to remote sensing problems. Methodological issues related to the use of these methods are summarized. Results from empirical studies applying fractal techniques are collected and discussed. Factors affecting the estimation of fractal dimension are outlined. Important issues for future research are also identified and discussed.

1. Introduction

Fractal geometry was introduced and popularized by Mandelbrot (1977, 1982) to describe highly complex forms that are characteristic of natural phenomena such as coastlines and landscapes. The main attraction of fractal geometry stems from its ability to describe the irregular or fragmented shape of natural features as well as other complex objects that traditional Euclidean geometry fails to analyse. In this sense, fractal geometry provides a new language in which previously intractable natural features can be described with more mathematical rigor (Barnsley 1989). Clarke and Schweizer (1991:p.37) note that 'Fractal geometry has been called one of the four most significant scientific concepts of the 20th century, on a par with quantum mechanics, the general theory of relativity, and the double-helix model of the structure of DNA.'

Fractal geometry has sparked considerable interest in the remote sensing community since the publication of Mandelbrot's book, *Fractals: Form, Chance and Dimension*, in 1977. The relevance and usefulness of fractal geometry to solving remote sensing problems can be attributed to the fact that remotely sensed images

International Journal of Remote Sensing
ISSN 0143-1161 print/ISSN 1366-5901 online
http://www.tandf.co.uk/journals
DOI: 10.1080/01431160600676695

are not only spectrally and spatially complex, but they often exhibit certain similarities at different spatial scales (Lam and De Cola 1993a). This requires us to examine spatially complex patterns with relatively simple indicators such as various measures of texture. It has been recognized that remotely sensed data can be analysed using five types of signature: spectral, spatial, temporal, angular, and polarization (Liang 2004). As more and more high spatial resolution imagery becomes available, utilization of spatial signatures plays an increasingly important role in extracting land surface properties from remotely sensed data. How to extract the complex and erratic textures in the image and use spatial information to improve image understanding and classification has been a major research issue in remote sensing for decades (Haralick *et al.* 1973, Weszka *et al.* 1976, Pratt *et al.* 1978, Gong and Howarth 1990, Wang and He 1990, Gong *et al.* 1992, Tso and Mather 2001). In this context, fractal geometry appears especially appealing because it offers something important, that is, tools for characterizing complex objects and land surface patterns in remotely sensed images.

Fractal models have been used in a variety of image processing and pattern recognition applications. For example, several researchers have applied fractal techniques to describe image textures and segment various types of images (Pentland 1984, Keller *et al.* 1989, De Jong and Burrough 1995, Myint 2003). Fractal characterization of the 'roughness' of remotely sensed images has been considered useful as part of the metadata of images or as a tool for data mining or change detection (Lam 1990, Jaggi *et al.* 1993, Emerson *et al.* 2004). Fractal models have also been used to study the scaling behaviour of geographic features and the knowledge generated by this type of research may be valuable for determining the optimum resolution of pixels and polygons used in remote sensing and GIS applications (Goodchild 1980, Lovejoy 1982, Mark and Aronson 1984, Emerson *et al.* 1999).

Applications of fractal techniques to image analysis rely heavily on the estimation of fractal dimensions. The fractal dimension, often denoted D, is a key parameter developed in fractal geometry to measure the irregularity of complex objects. A variety of methods have been proposed to compute the D of features such as topographic surfaces and image intensity surfaces. However, most computational methods have their theoretical and/or practical limitations. Several studies (Roy *et al.* 1987, Tate 1998, Lam *et al.* 2002, Sun 2006, Sun *et al.* 2006) have reported that different methods often yield significantly different D values for the same feature. In addition to method-induced errors, a number of other factors such as the choice of input parameter values and image data used may also influence computed D values. As such, there is considerable uncertainty regarding the nature and extent of variations in computed D.

Despite these developments, there has been no review paper summarizing and evaluating different methods and applications that are widely scattered in the literature. The purpose of this paper is to provide a survey of commonly used methods for estimating fractal dimension and their applications to the analysis of remotely sensed images. The focus of our discussion is on the methodological issues related to the practical measurement of D in the remote sensing context. Contrasting or conflicting results from empirical studies are collected and discussed. Major factors influencing the computed D are outlined. Important issues for future research are also identified and discussed. The next section provides a brief introduction to the basic concepts of fractal geometry, followed by a description of six computational methods. Examples illustrating applications of fractal techniques in remote sensing are then presented. Major issues encountered in fractal analysis of remotely sensed images are finally discussed. We conclude the paper with some general remarks.

2. Fractals, self-similarity, and the fractal dimension

'Clouds are not spheres, mountains are not cones, coastlines are not circles, and bark is not smooth, nor does lightning travel in a straight line…' (Mandelbrot 1982:p.1). Nature is complex. Many important features and patterns of nature are so irregular that classical Euclidean geometry is hardly of any help in describing their form. It was this inability of classical geometry to describe the real world that led Mandelbrot (1977) to invent the concept of 'fractal' to fill the void caused by the absence of suitable geometric representation for a family of shapes that are continuous but not differentiable.

According to Mandelbrot (1977:p.4), the term *fractal* comes from the Latin adjective *fractus*, which is also the root for *fraction* and *fragment* and means 'irregular or fragmented'. Formally, a fractal is defined as a set for which the Hausdorff-Besicovitch (or fractal) dimension strictly exceeds the topological dimension (Mandelbrot 1977). A fundamental characteristic of fractal objects is that their measured metric properties, such as length or area, are a function of the scale of measurement. A classical example to illustrate this property is the 'length' of a coastline (Richardson 1961, Mandelbrot 1967). When measured at a given spatial scale δ, the total length of a crooked coastline $L(\delta)$ is estimated as a set of N straight-line segments of length δ. Because small details of the coastline (e.g. peninsulas) not recognized at lower spatial resolutions become apparent at higher spatial resolutions, the measured length $L(\delta)$ increases as the scale of measurement δ increases. Thus, in fractal geometry, the Euclidean concept of 'length' becomes a process rather than an event, and this process is found to be controlled by a constant parameter (Richardson 1961). Mandelbrot (1967, 1977) generalized and expanded on Richardson's (1961) empirical findings and showed that the relationship between length and measuring scale can be described by the power law:

$$L(\delta) = K\delta^{(1-D)}, \tag{1}$$

where the exponent D is called the fractal dimension, and K is a constant.

The scaling exponent D in equation (1), i.e. the fractal dimension, is a central construct of fractal geometry. It is called *fractal* dimension because it is a *fractional* (or non-integer) number (Mandelbrot 1977). The idea of using D to describe irregular shapes is a powerful one because it captures what is lost in traditional geometrical representation of form. In Euclidean geometry, dimensions are integers or whole numbers (e.g. 1 for lines, 2 for areas, and 3 for volumes), and topological dimensions remain constant no matter how irregular a line or an area may be. Thus, a straight line and a crooked coastline have the same topological dimension 1, and a smooth surface and a rugged topographic surface have the same topological dimension 2. In other words, topology cannot discriminate between crooked lines and straight lines (Mandelbrot 1982). As such, part of the information about the form of irregular objects is necessarily lost in topological representations.

In fractal geometry, on the other hand, dimension is treated as a continuum. A curve's dimension, for example, can take on any non-integer value between 1 and 2, depending on the degree of irregularity of its form. The more contorted a line is, the higher its dimension. Similarly, a surface's dimension may be a non-integer value between 2 and 3. The use of a fractional power in the description of complex shapes compensates, in effect, for the length or area lost because of details smaller than the measurement scale (δ). With D it becomes possible to obtain consistent estimates of an object's metric properties at different measurement scales (Pentland 1984).

Fractal dimension can be thought of as a measure of an object's ability to 'fill' the space in which it resides. A smooth line of $D=1$ will approach $D=2$ when it becomes so complex that it effectively takes up the whole plane. Similarly, as a surface's D approaches the upper value 3, it will appear increasingly rugged and display a rapid succession of peaks and valleys. More generally, the more irregular an object becomes, the more space it fills, and the higher its D value. In this way, the value of D is intimately linked to our notion of 'complexity' or 'roughness' (Pentland 1984).

Self-similarity is another key property of fractals. Formally, self-similarity is defined as a property where a subset, when magnified to the size of the whole, is indistinguishable from the whole (Mandelbrot 1977, Voss 1988). The property of self-similarity implies that the form of an object is invariant with respect to scale. In other words, a strictly self-similar object can be thought of as being constructed of an infinite number of copies of itself. In the geosciences, the property of self-similarity may be better termed scale-independence (Clarke 1986). The forms of natural phenomena are often erratic as 'chances' or random factors often play an important role in their generating processes (Mandelbrot 1977). As such, unlike mathematical fractals, natural objects generally do not display exact self-similarity. Instead, they may exhibit a certain degree of statistical self-similarity over a limited range of scales. Statistical self-similarity refers to scale-related repetitions of overall complexity, but not of the exact pattern (Voss 1988).

Self-similar objects are isotropic (or rotation invariant) upon rescaling. If rescaling of an object is anisotropic, then the object is said to be self-affine. Formally, with self-affine fractals the variation in one direction scales differently than the variation in another direction (Mandelbrot 1985). Thus, the trail of particulate Brownian motion in two-dimensional space is self-similar, whereas a plot of the x-coordinate of the particle as a function of time is self-affine (Brown 1995). Similar to the concept of statistical self-similarity, an object is said to be statistically self-affine if it displays self-affinity only in a statistical sense.

Fractals, self-similarity, and fractal dimension are the key concepts of fractal geometry upon which most remote sensing applications seem to have drawn. The relevance of these concepts to the analysis of remotely sensed images will be discussed in greater detail in the following sections. The reader is referred to Mandelbrot (1977, 1982) for a more complete discussion of fractal geometry. For an introduction to fractal analysis of images, the reader is directed to Peitgen and Saupe (1988). An excellent introduction to fractals in geography can be found in Lam and De Cola (1993a). The review of fractals in physical geography presented by Gao and Xia (1996) is also informative.

It should be noted that, although this paper focuses on the current state of fractal analysis techniques in Earth imaging, fractal geometry has found application in a wide range of scientific fields (Dyson 1978). For example, fractal models have been used extensively in pattern recognition (e.g., Peleg *et al.* 1984, Dennis and Dessipris 1989, Chaudhuri *et al.* 1993, Blacher *et al.* 1993). Fractal geometry has contributed much to computer science (e.g. Peitgen and Richter 1986, Devaney and Keen 1989).

In computer graphics, fractal techniques have been used, for example, to simulate realistic landscapes such as rugged terrains, which can be used in motion pictures and flight simulators (Fournier *et al.* 1982). Fractal geometry has also been applied to such diverse fields as meteorology (Lovejoy and Schertzer 1985, 1990), ecology (Loehle 1983, Wiens 1989), material science (Lu and Hellawell 1995), urban landscapes (Batty & Longley 1986), economics and finance (Calvet and Fisher 2002, Mandelbrot and Hudson 2004), soil sciences (Burrough 1981, Armstrong 1986, Green and Erskine 2004), and medical imaging (Chen *et al.* 1989, Wu *et al.* 1992, Lee *et al.* 2003). Readers interested in the works done outside the Earth imaging realm should consult major journals in fields of interest.

3. Methods to compute the fractal dimension of image intensity surfaces

The fractal dimension of strictly self-similar objects can be derived mathematically and is given by (Mandelbrot 1977):

$$D = \frac{\log(N_r)}{\log(1/r)}, \tag{2}$$

where N_r represents an object of N_r parts scaled down by a ratio of r. The D derived from equation (2) is called the shape's similarity dimension (Mandelbrot 1977).

For non-mathematical objects, however, the fractal dimension cannot be derived analytically. Instead, it must be empirically estimated. A large number of methods have been proposed to compute the fractal (monofractal) dimension of natural objects. These methods differ in the ways they approximate the quantity N_r in equation (2), but they are similar in spirit in that they use some version of the statistical relationship between the measured quantities of an object and step sizes to derive the estimates of D. The 'quantity' of an object is expressed in terms of, for example, length, area, or number of boxes (cells) needed to cover the object. 'Step size' refers to the scale or resolution of measuring units used. The procedure common to most of the methods discussed in this paper consists of three steps:

- First, measure the quantities of the object under consideration using various step sizes.
- Second, plot log (measured quantities) versus log (step sizes) and fit a least-squares regression line through the data points. The log–log plot is often referred to as the Richardson plot.
- Third, use the slope of the regression line to derive the D of the object.

A remotely sensed image can be viewed as a hilly terrain surface whose 'elevation' is proportional to the grey level or digital number (DN) value. As such, all methods developed to compute the D of surface features can, in principle, be readily applied to remotely sensed images. Broadly, there are two basic approaches for computing the D of surfaces. The first is to directly estimate D from the surfaces being analysed. The second approach involves the so-called dimensionality-reduction technique (Klinkenberg 1994). In this approach, the D of a surface is estimated by first calculating the D of contours or profiles extracted from the surface and, then, simply adding 1 to account for the different Euclidean dimension. In this section, we describe six methods for computing the D of *surface* features such as remotely sensed images. For a review of the methods used to calculate the D of *linear* features, the reader is directed to Klinkenberg (1994).

3.1 *The triangular prism method*

The triangular prism method was developed by Clarke (1986) primarily to calculate the *D* of topographic surfaces, but it has been applied extensively to remotely sensed images. The method makes use of a raster representation of the elevations of the Earth's surface such as in a digital elevation model (DEM) (see figure 1 (a and b)). Based on this data structure, the method takes elevation values (or the equivalent of DN value in an image) at the corners of squares (i.e. analysis windows) (*a*, *b*, *c* and *d* in figure 1a), interpolates a centre value (*e* in figure 1(a)), divides the square into four triangles (*abe*, *bce*, *cde* and *dae* in figure 1(b)), and then computes the top surface areas of the prisms which result from raising the triangles to their given elevations (*A*, *B*, *C*, and *D* in figure 1(a)). By repeating this calculation for geometrically increasing square sizes (δ), the relationship between the total upper surface area of the prisms (i.e. the sum of areas *A*, *B*, *C*, and *D* in figure 1(a)) and the spacing of the squares (i.e. step size δ) can be established, and used to estimate *D* (table 1). The only input parameter required by this method is the number of step sizes. Generally, the method is less computationally intensive than other methods such as the variogram or Fourier power spectrum methods (Clarke 1986).

Several modifications have been proposed since Clarke (1986) presented his method. In Clarke's original algorithm, 'spacing of the square' was interpreted as 'area of the square.' In other words, Clarke used step size squared (δ^2) in the

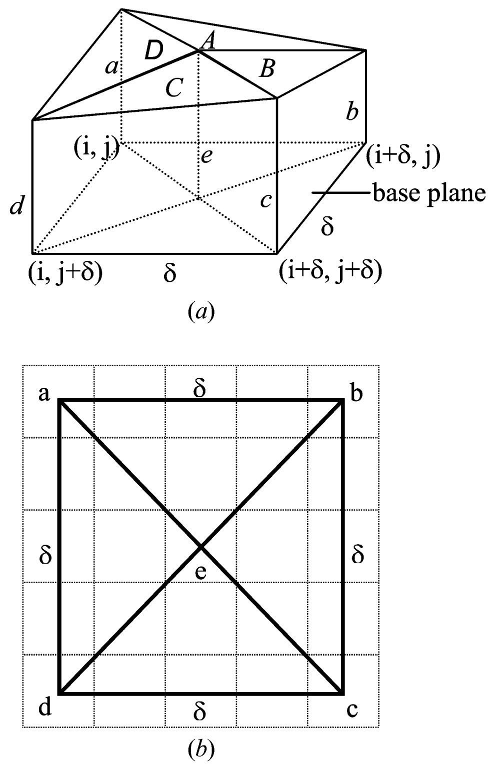

Figure 1. (*a*) 3D view of the triangular prism method (after Clarke, 1986); (*b*) Top view of the corner pixels (*a*, *b*, *c*, and *d*) and the centre point (*e*) used in Clarke's (1986) method (an example with step size = 4).

Table 1. Methods for computing the fractal dimension (D) of surface features†.

Method	Relation used	Basic formula	Estimate of D
Triangular prism	Total area of the tops of prisms vs. side length of analysis windows	$S(\delta) \propto \delta^{2-D}$ $S(\delta)$=area δ=side length of analysis windows	Plot log $S(\delta)$ versus log (δ), slope is $(2-D)$ $D=2-$slope
Differential box counting	Number of boxes needed to cover an image vs. box size	$N_r \propto (1/r)^{-D}$ N_r=number of boxes $r=s/M$, s=side length of boxes, M=side length of the image	Plot log N_r versus log $(1/r)$, Slope is $-D$ $D=-$slope
Variogram	Mean squared elevation (or DN) difference vs. distance	$E[(Z_p-Z_q)^2] \propto (d_{pq})^{2H}$ Z_p, Z_q=elevations or DNs at points p and q d_{pq}=distance between p and q	Plot log $\{E[\ldots]\}$ versus log d_{pq} slope is $2H$ $D=3-H=3-$slope/2
Isarithm	Length of contour line vs. step size	$L(\delta) \propto \delta^{1-D_{\text{contour}}}$ $L(\delta)$=length of contour line (i.e., number of boundary cells) δ=step size	For each contour line, plot log $L(\delta)$ versus log (δ), slope is $(1-D_{\text{contour}})$ D=average of all $D_{\text{contour}}+1$
Robust fractal estimator	Length of profile vs. step size	$L(\delta) \propto \delta^{1-D_{\text{profile}}}$ $L(\delta)$=length of profile δ=step size	For each cell, take the average of D_{profile} in both EW and NS directions D obtained by combining fractal dimensions of each cell using a weighted average and adding 1
Power spectrum	Fourier power spectral density vs. the frequency	$P(f) \propto f^{-(5-2D_{\text{profile}})}$ $P(f)$=power, f=frequency	Plot log $P(f)$ versus log (f), slope is – $(5-2D_{\text{profile}})$ $D=D_{profile}+1$

†D_{contour}=fractal dimension of a contour line; D_{profile}=fractal dimension of a profile. For references see §3 of the text.

regression. Lam *et al.* (2002) have shown that step size (δ) instead of step size squared (δ^2) should be used to derive the correct D. Sun (2006) has recently proposed three new procedures to implement the triangular prism method. Sun's methods differ from Clarke's method in that, in constructing the prisms, they take into account the actual DN values of all the pixels at the edges of an analysis window. Sun (2006) reported that her methods perform better than Clarke's (1986) original method when applied to images with complex textures.

Clarke (1986) reported that the triangular prism method provided good results for the test data used in his work. Clarke and Schweizer (1991) found that subsequent tests of the method on terrain data have yielded rather low D values. In a systematic study comparing the performance of several methods, Lam *et al.* (2002) showed that the triangular prism method was the best estimator for rougher surfaces with generated D=2.9 and 2.7, although it was less accurate where generated D=2.5 and 2.3. They also found that the triangular prism method was sensitive to contrast stretching and recommended that, to ensure comparability and accuracy of measurement, the range of DN values of an image be normalized before using the method. The triangular prism method was also found to be sensitive to 'noise' or extreme grey level values (Qiu *et al.* 1999). To obtain reliable results, it is important first to assess whether the image to be measured has any noisy pixels before applying the method.

3.2 *The differential box-counting (DBC) method*

The differential box-counting (DBC) method was proposed by Sarkar and Chaudhuri (1992) to compute the D of digital images. This method can be thought of as a variant of the well-known box-counting approach (Goodchild 1980, Voss 1988). In the differential box-counting method, N_r in equation (2) is counted in the following manner. If an image of size $M \times M$ pixels is scaled down to a size $s \times s$ where $M/2 \geqslant s > 1$ and s is an integer, then we have a ratio of $r = s/M$. Consider the image as a 3D space with (x, y) denoting the image plane and (z) denoting the grey level. The (x, y) space is partitioned into grids of size $s \times s$. On each grid there is a column of boxes of size $s \times s \times s'$. If G denotes the grey level range of the image (e.g. 256), s' is calculated by $[G/s'] = [M/s]$. Let the minimum and maximum grey level of the image in (i, j)th grid fall in box number $z_{\min}$ and $z_{\max}$, respectively. Then $n_r(i, j) = z_{\max} - z_{\min} + 1$ is the contribution of N_r in (i, j)th grid. Taking contributions from all grids, we have:

$$N_r = \sum_{i,j} n_r(i, j) \tag{3}$$

For different values of r, that is, different values of s or step sizes, the quantity N_r is counted. D then is computed from the least-squares linear fit of log (N_r) versus log ($1/r$) (table 1).

Sarkar and Chaudhuri (1992) have shown that the DBC method is both accurate and computationally efficient. Despite this, the method does not seem to have been widely applied to remote sensing problems (Tso and Mather 2001). One possible explanation for the lack of interest in this method among remote sensing researchers is that the method was developed outside the geosciences domain. It remains to see how effective the DBC method is when applied to remotely sensed images.

3.3 *The variogram method*

The variogram method is a widely used technique for computing *D* of surfaces. In this method, the mean of the squared elevation (or DN) difference (i.e. variance) is calculated for different distances, and *D* is estimated from the slope (*b*) of the regression between the logarithms of variance and distance (see figure 2) so that $D=3-b/2$ (Mark and Aronson 1984; see also table 1). Variations of the variogram method exist. Roy *et al.* (1987), for example, calculated *D* using four different implementations of the variogram method.

Because of its ease of use, the variogram method has been used in numerous studies (Goodchild 1980, Burrough 1981, Mark and Aronson 1984, Roy *et al.* 1987, Carr and Benzer 1991, Klinkenberg and Goodchild 1992). Lam and De Cola (1993b) noted that three other properties of the variogram method may have also contributed to its popularity. First, the method can be applied to both regular and irregular data. Second, for irregular polygonal data, the variogram function can be determined by centroids representing the polygons. Third, when compared with the isarithm method (discussed in §3.4), the variogram method is generally more reliable.

The variogram method is based on the assumption that the surface being analysed is a fractional Brownian surface. Studies of natural terrain surfaces (Mark and Aronson 1984, Roy *et al.* 1987) have shown, however, that variograms often do not behave linearly at all scales, suggesting that natural phenomena are not truly fractal (discussed in §5.1). Another issue that requires attention in variogram analysis is the sampling strategy used to determine the point pairs. Klinkenberg (1994) suggested that, for statistical reasons, the sample of point pairs uniformly span the distance range of a given dataset and the distance classes be constructed so that they are evenly spaced in the log–log space used in the regression. Furthermore, while the shortest point-pair distance will depend on the resolution of the data used, attention should be given to the choice of the maximum point-pair distance. The common practice is to use one-half of the absolute maximum distance between points of a given dataset as the maximum point-pair distance. Roy *et al.* (1987) have suggested using even shorter maximums, such as one quarter the maximum distance. Klinkenberg (1994) argued, however, that the rule of using one-half or one quarter of the maximum distance as the maximum point-pair distance appears more restrictive than necessary.

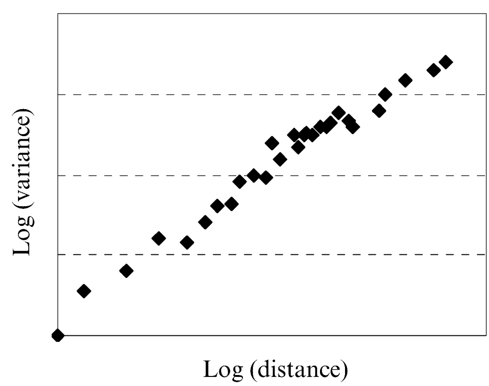

Figure 2. The log (variance) versus log (distance) plot used in the variogram method.

Different studies reached different conclusions regarding the performance of the variogram method. Klinkenberg and Goodchild (1992), for example, found that the variogram method was able to produce consistent estimates of D when applied to topographic data. Clarke and Schweizer (1991), on the other hand, reported that for the same dataset, the variogram method appears to yield consistently higher D values than those obtained from the triangular prism method and the robust fractal estimator (discussed in §3.5). The work of Lam *et al.* (2002) suggests that the variogram method was a comparatively poor estimator for all the simulated surfaces used in their study. One major limitation of the variogram method is that remotely sensed images are data rich and exhaustive. In order to make the variogram method computationally tractable, studies applying the variogram method to image analysis use random sampling of a subset of pixels. This makes the computed D a random variable that changes from one analysis to the next.

3.4 *The isarithm method*

The isarithm method (Shelberg *et al.* 1983) is based on the premise that the complexity of isarithm or contour lines may be used to approximate the complexity of a surface. Briefly, the method works in the following way. Starting with a matrix of z-elevations (or DN values), an isarithm interval is selected and isarithm lines are constructed on the surface. For each isarithm line, its lengths are calculated in terms of the number of boundary cells over a number of step sizes, log (number of boundary cells) is regressed against log (step sizes), and the slope of the regression line is used to derive the D of the isarithm line. This process is repeated for every isarithm line. The surface's D is obtained by averaging the D values of all the isarithm lines that have $R^2 \geqslant 0.9$ and adding 1 (table 1).

To implement the isarithm method, a data matrix of a given number of rows and columns must be specified, with the following parameter input by the user: (1) the number of step sizes, (2) the isarithm interval, and (3) the direction in which the computation is implemented (row, column or both). It is possible that for a given step size, there are no boundary cells. In this case, the isarithm line is excluded from the analysis to avoid regression using fewer points than the given number of steps (Shelberg *et al.* 1983). Lam (1990) pointed out that this feature appears especially useful for the analysis of remotely sensed images as it ensures that random noise in the image will not be taken into account in the estimation process.

Lam and De Cola (1993b) have discussed several factors that may influence the computed D values using the isarithm method. They noted that real data are generally anisotropic and, therefore, the computed D will vary depending on whether it is measured along rows, columns, or in a non-cardinal direction. The maximum step size used may also affect the reliability of estimation results. Furthermore, the practice of using the average of the D values of those isarithm lines that have $R^2 \geqslant 0.9$ to represent the surface D is somewhat arbitrary.

Shelberg *et al.* (1983) pointed out that an advantage of the isarithm method is that, by using a number of isarithm lines, the method can be used to estimate the D for non-self-similar surfaces. Furthermore, the method was found to be robust to random noise in the image (Qiu *et al.* 1999). Clarke (1986), however, seemed quite critical of the isarithm method and commented that, 'This method is rather crude, however, and really is an empirical estimate of an empirical estimate' (p.714). Despite this, the isarithm method appears to be one of the most often used methods for computing the D of remotely sensed images (Lam 1990, Lam and De Cola 1993b, Qiu *et al.* 1999, Emerson *et al.* 1999, Lam *et al.* 2002). Applications of the isarithm method have shown that the method returned good results for images with medium-ranged complexity, but it overestimated D when applied to rougher surfaces while it underestimated D for smooth images (Emerson *et al.* 1999, Lam *et al.* 2002).

3.5 *The robust fractal estimator*

The robust fractal estimator was proposed by Clarke and Schweizer (1991) in an attempt to provide stability in the computation of D. Using the walking-dividers method, the robust fractal estimator computes for each cell the D of each profile in both the east–west and north–south directions and places the average of the two in a new array. The D of the entire surface is obtained by combining the D values of each cell using a weighted average and adding one (Clarke and Schweizer 1991).

Clarke and Schweizer (1991) noted that the robust fractal estimator is primarily designed to calculate D for natural surfaces using data from USGS DEMs, but it should work equally well on any gridded surface data. Applications of this estimator to image analysis seem limited, however. As such, little is known about its performance. In their paper, Clarke and Schweizer reported that for the same datasets used in their study, the robust fractal estimator appeared to consistently yield a lower D value than those obtained from the triangular prism and variogram methods. In a discussion of how to select the largest step size when using the divider method on self-affine curves, Klinkenberg (1994) pointed out that the low estimated D values (close to one) reported in Clarke and Schweizer (1991) may be due to the fact that they used steps sizes that spanned the crossover length. Note that the crossover length refers to the range of scale within which the computed D is representative of the local fractal dimension of a self-affine feature. Discussion of the crossover length concept can be found in Mandelbrot (1985).

3.6 *The Fourier power spectrum method*

Another technique for computing the D of surface features is the use of Fourier analysis. The Fourier method uses the power spectrum derived from the surface (Pentland 1984, Burrough 1981). It can be shown that the Fourier power spectrum $P(f)$ of a fractional Brownian function (f) is proportional to $f^{(-2h-1)}$, where $h=2-D_{\text{profile}}$ (Pentland 1984). The fractal dimension of the profile (D_{profile}) is obtained from the slope of the regression line of the log-log plot of $P(f)$ versus f. The D of the surface is computed as $D=D_{\text{profile}}+1$ (table 1). Detailed descriptions of the steps required to perform a spectral analysis for fractal applications can be found in Peitgen and Saupe (1988) and Turcotte (1992).

Spectral methods should only be applied to self-affine curves (i.e. profiles) since they will always return a $D=1$ for self-similar curves (Peitgen and Saupe 1988). Several researchers (Fox and Hayes 1985, Clarke 1986, Carr and Benzer 1991) have pointed out that, although a rigorous method, the power spectrum method involves sophisticated data preprocessing and is computationally complex, a fact that appears to have limited its applications. The inherent complexity of spectral methods requires that they be carefully implemented (Klinkenberg 1994).

4. Applications of fractal techniques to remote sensing image analysis

There is a large amount of literature on the applications of fractal techniques to the analysis of remotely sensed images. A main thrust in this application literature is the use of D to measure the roughness or textural complexity of land surface features. In this paper, we focus on four major application areas: that is, the use of computed D (1) to characterize the overall spatial complexity of an image, (2) to supply image classification with textual information, (3) to describe the geometric complexity of the shape of feature classes in a classified image, and (4) to examine the scaling behaviour of environmental phenomena. We provide below a review of representative works published in each of these four application areas.

4.1 *Using* D *to characterize the overall spatial complexity of remotely sensed images*

Perhaps the most obvious utility of fractal models in image analysis is the use of D to characterize the overall textural complexity of remotely sensed imagery (Lam 1990, Qiu *et al.* 1999, Read and Lam 2002, Weng 2003). In these applications, only a single D for the entire image is computed. Such a global D can be calculated for remotely sensed data of different land cover types, sensors, and bands. Lam (1990), for example, used the isarithm method to measure the spatial complexity of three Landsat TM images representing three different land cover types in coastal Louisiana. She found that the estimated D values of these TM surfaces were generally higher than those of most real-world terrain surfaces. Among the three land cover types, the highest D occurred in an urban area, followed by a complex coastal area and a rural area. She also compared the D values of the three land cover types across seven spectral bands and found that the D values of the same land cover type turned out to be quite different in different bands. The urban landscape has its highest D values occurring in bands 2 and 3, whereas the coastal and rural areas both exhibit high D values in band 1. Lam (1990) noted that, although the three land cover types examined in her study appeared to have different D values, the difference in the average D values among the three land cover types was small compared to the differences in overall D values among bands.

In an analysis of two AVIRIS (Airborne Visible Infra-Red Imaging Spectrometer) images of the Los Angeles area, Qiu *et al.* (1999) found that the computed D values for urban landscapes were higher than those for rural landscapes. A novel part of this study was the systematic comparison of the computed D values of the two study areas across the full spectral range of the hyperspectral images (224 bands). They confirmed Lam's (1990) finding that the textural complexity of the same land cover type, expressed as D values, varied significantly across bands. They found that higher contrast in D values between the urban and rural landscapes occurred in the visible bands. They also reported unusually high D values ($D>2.9$) detected in the spectral bands where signal-to-noise ratios were low. An important finding of Lam (1990) and Qiu *et al.* (1999) studies is that the texture of a land cover type may be better characterized by certain band(s) than by others. As such, identifying the bands in which the contrast in computed D between different land cover types is most distinct may be a necessary step in dealing with multispectral images.

Fractal techniques have also been used to describe spatial variations of environmental phenomena along certain transects extracted from remotely sensed images. In a study of the urban heat island effect in a Chinese city, Weng (2003) applied fractal techniques to analyse the spatial variability of surface radiant temperature along three profiles constructed from Landsat TM images. His results suggest that variations in estimated D values along a profile can be linked to underlying land cover types. He also compared D values across several years and between different seasons of the year. His results show that information about inter-temporal changes in D values was useful in understanding the increased textural complexity of the thermal surfaces as well as the seasonal dynamics of urban heat island effect.

Fractal characterization of the overall complexity of remotely sensed images has been considered useful as part of metadata or as a tool for data mining and change detection (Jaggi *et al.* 1993, Lam *et al.* 2002, Emerson *et al.* 2004). An advantage of the fractal technique in these applications is that global D values can be computed without the need to first classify the image. Given the rapidly increasing types and volumes of remotely sensed data available today, quantitative assessment of the spatial characteristics of various images may become a useful exercise in selecting the right data for a particular application. Another potential utility of fractal characterization of remotely sensed data is the use of D as an initial screening tool for examining information content contained within different spectral bands. Variations in D values across bands may be used as a guideline for identifying noisy bands or for the selection of bands for image display, classification, and analysis (Lam 1990, Qiu *et al.* 1999). Such information may be particularly valuable for applications where texture is important.

4.2 *Use of* D *as a texture measure to segment and classify images*

The use of only spectral signatures to distinguish land cover types has proved inadequate. Numerous studies have shown that classification results may improve if additional information about spatial variations in pixel values is incorporated in the classification procedure. Many techniques, such as co-occurrence matrices (Haralick *et al.* 1973), local variance (Woodcock and Strahler 1987), wavelets (Mallat 1989) and spatial autocorrelation statistics (Cliff and Ord 1973), have been proposed to extract textural information from remotely sensed images.

Fractal techniques appear well suited to the analysis of textural features in remotely sensed images, as the environmental features captured in the image are often complex and fragmented (Burrough 1981, Lorimer *et al.* 1994). It has been suggested that local variations in computed D can be used as texture measures to segment images (Pentland 1984, Keller *et al.* 1987). The idea is that different land cover types may have characteristic textures or roughness that could be described by different D values. Ideally, if there were a one-to-one relation between the texture of a land cover type and a unique D value, then the D could be viewed as the 'fractal signature' of that land cover type and used to extract it from the image.

Pentland (1984) pioneered the use of fractal geometry in image texture analysis and segmentation. In his 1984 paper, Pentland considered the image intensity surface as a fractal Brownian function (fBf) and estimated D from Fourier power spectrum of fBf. He segmented several types of images using computed D values and achieved good results. He also found that the computed D was always stable over at least 4 : 1 variations in scale, and most segmentations were stable over a range of 8 : 1. He concluded that fractal-based image segmentation appeared to be a powerful technique (Pentland 1984).

Perhaps the best example illustrating the utility of fractal techniques in image classification was presented by De Jong and Burrough (1995). In their study, De Jong and Burrough proposed a so-called 'local D algorithm,' a method that can be thought of as a local implementation of the triangular prism concept (Clarke 1986). In the 'local D algorithm,' a kernel of 9 by 9 pixels is moved over the image and, at each position of the kernel, a D is computed within the kernel, resulting in a new image file containing the estimated local D values. This new layer of D values was then used as texture measures in the classification procedure. De Jong and Burrough applied their method to the classification of six Mediterranean vegetation types in two remotely sensed images. The results from the analysis of these two images seem somewhat mixed. While the 'local D algorithm' appeared effective in separating five of the six land cover types in a Landsat TM image, the method could not sharply distinguish between any of the six land cover types when applied to an airborne GER (Geophysical Environmental Research Imaging Spectrometer) image. This poor result was explained by the poor quality of the GER image. They concluded that, although local D values for TM imagery seemed to reflect the different land cover types examined in their study, D values by themselves were insufficient for the classification of TM images.

Other studies attempting to gauge the usefulness of fractal techniques for image classification purposes include Jones *et al.* (1989), Keller *et al.* (1989), LaGro (1991), De Jong (1993), Myint (2003) and Sun (2006), among others. In a comprehensive study comparing the discriminatory power of several texture analysis methods, Myint (2003) found that the spatial autocorrelation approach (Moran's I and Geary's C) was superior to fractal approaches (isarithm, triangular prism, and variogram) and, in some cases, simple standard deviation and mean value of the samples gave better classification accuracies than all or some of the fractal techniques. His results also show that the computed D values for the same image vary with the computational method and spectral band used. He concluded that fractal-based textural discrimination methods are applicable but these methods alone may be ineffective in identifying different land cover types in remotely sensed images.

It should be noted that, when used to analyse local tonal variations in the image (i.e. local D values), fractal techniques provide meaningful results only for image portions larger than the smallest step size used. In other words, texture variations at scales smaller than the smallest step size will be overlooked in fractal analysis. This is often referred to as the blurring effect. How to choose an 'appropriate' window size and how to deal with the boundary effect, as well as the blurring effect, are two important issues that deserve attention in computing local D values. These issues will be discussed in greater detail in §5.5.

4.3 *Fractal characterization of classified image features*

Fractal analysis has been shown to be of descriptive value in the analysis of spatial complexity of classified image features. Lovejoy (1982), for example, analysed the perimeter–area relationship of rain and cloud areas identified from satellite and radar images. He found that the degree of contortion of the perimeter of cloud regions could be described by $D=1.35$ over a range of cloud sizes from less than $1\,km^2$ to over $10^6\,km^2$. A more comprehensive example of fractal description of classified image features was presented by De Cola (1989). In his study, De Cola used the perimeter–area relationship to describe the shape of regions of eight land cover classes extracted from a Landsat TM image of north-west Vermont. He showed that it was possible to associate land cover types with D values. For example, the forests examined in his study were characterized by high D and large regions, while agricultural activities had large regions with D inversely related to the intensity of cultivation, and urban land-use yielded small regions with relatively high D.

Fractal description of classified image features can provide useful descriptive statistics for characterization of the aggregate feature classes. Knowledge about the characteristic D values of different feature classes may be valuable in understanding the processes that generate the phenomena under consideration (Lovejoy 1982). Another utility of fractal description of classified image features is the use of such data as input to GIS. De Cola (1989) demonstrated how the analysis of individual land cover regions, such as the urban regions in his study, can provide a raster-based GIS data structure and be used to investigate the location and description of individual regions and to check the reliability of classification and labelling processes.

4.4 *Scaling characteristics of remotely sensed images*

Most research published to date has suggested that real remotely sensed images are not true fractals (discussed in §5.1). This finding is clearly in violation with the assumption underlying the fractal model, i.e. the objects under consideration are self-similar, at least statistically. Some researchers (e.g. Lam *et al.* 2002) have argued, however, that lack of self-similarity in real remotely sensed data could be used positively. Given that the estimated D is stable only over limited ranges of scale, the behaviour of D can be used to study the effects of scale changes on image properties. Several studies have examined the scaling properties of digital images (Lovejoy 1982, Pentland 1984, Emerson *et al.* 1999, Lam *et al.* 2002, He *et al.* 2002). A good example of the research in this direction was provided by Emerson *et al.* (1999). In their study, Emerson *et al.* examined the effect of changing pixel size on the computed D values of NDVI (Normalized Difference Vegetation Index) images of two study areas. In the example of Huntsville Alabama, they found that the estimated D values of NDVI images of agriculture, forest, and urban areas responded differently to aggregation. The image of the agricultural area grew more complex as the pixel size was increased from 10 to 80 m, while the forested area grew slightly smoother and the complexity of the urban area remained approximately the same. The analysis of the image data of the East Humboldt Range in Nevada showed a more complex relation between pixel size and D and this relation changes between seasons.

Emerson *et al.* (1999) pointed out that information about the scaling behaviour of environmental phenomena may be valuable for the selection of an optimal resolution for characterizing the phenomena under investigation. For example, environmental phenomena that are more scale independent may require fewer data or lower resolutions than those that are highly scale dependent. They also argued that the response of D values to scale changes may be used as a guide to identify the scale at which the processes that produced certain phenomena operate.

In addition to the four major application areas discussed above, there are other applications that are not reviewed here. For example, fractal techniques have been applied to image simulation (Pachepsky *et al.* 1997, Ricotta and Avena 1998, Ricotta *et al.* 1998), image compression (Belloulata and Konrad 2002), image denoising (Ghazel *et al.* 2003), image filtering (Germain *et al.* 2003), characterization of the structures of hydrological basins (Maitre and Pinciroli 1999), and so forth.

5. Discussion and research need

Remotely sensed images with different textural characteristics are expected to have different D values. However, differences in image texture are not the only factor influencing the computed D (figure 3). This raises the question of what is actually

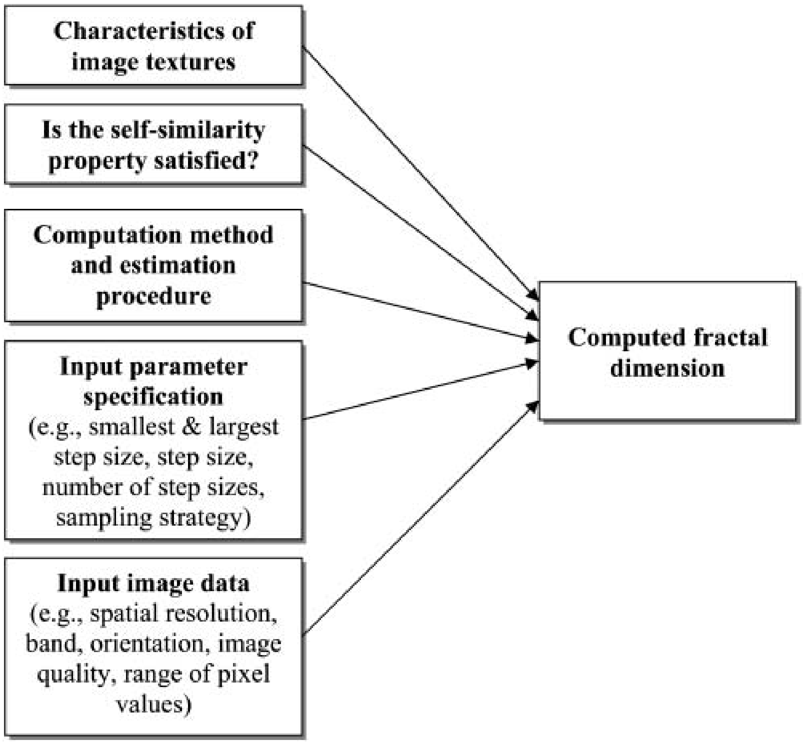

Figure 3. Factors influencing the computed fractal dimension of remotely sensed images.

captured in the computed *D*. In this section, we discuss the major sources of limitations and uncertainty in the application of fractal techniques in remote sensing. The focus of our discussion will be on several issues common to the methods and applications discussed above. Following a brief discussion of each of these issues, we offer our thoughts on the research potential for fractals in remote sensing.

5.1 *Are remotely sensed images fractal?*

The self-similarity property underlying the fractal model predicts that for truly fractal surfaces, the computed *D* should be constant at all scales, at all locations, and in all directions. Numerous studies have shown that the estimated *D* values of most natural phenomena are unstable with respect to scale, location, and/or orientation (Mark and Aronson 1984, Roy *et al.* 1987, Klinkenberg and Goodchild 1992, Burrough 1993). The consensus that has emerged from the research published to date is that, as far as natural phenomena are concerned, self-similarity is exhibited only in a statistical sense and such statistical self-similarity, when present, is exhibited only in limited regions and over limited ranges of scale (Goodchild and Mark 1987, Milne 1991).

Are remotely sensed images fractal? Studies directly addressing this issue appear scarce. Nevertheless, a number of studies have found that the estimated *D* of real remotely sensed images vary with the resolution of the image used and the region and direction in which *D* was computed (Lam 1990, Emerson *et al.* 1999, De Jong and Burrough 1995, Lam *et al.* 2002, Sun *et al.* 2006). De Jong and Burrough (1995) have further noted that the log–log plots constructed in their study were nonlinear beyond a certain range, indicating breaks in the slope of the regression lines and hence the *D*. These results suggest that most remotely sensed images are not strictly self-similar; instead, they may be at most only statistically self-similar over a limited range of pixel sizes.

The observation that most remotely sensed images may not be even statistically self-similar brings up an important issue, i.e. does it make sense to use *D* to describe image textures? At the theoretical level, lack of self-similarity does violate the assumptions underlying most of the methods discussed in §3. For example, the variogram method assumes that the surfaces being analysed have statistical properties similar to those of fractal Brownian surfaces. If this were not the case, then the method would not necessarily yield a correct *D* (Piech and Piech 1990). However, some researchers have suggested that lack of self-similarity is not a limitation to the fractal technique and it could be simply seen as a method for extracting information from the Richardson plot (Orford and Whalley 1983, Kennedy and Lin 1986, Normant and Tricot 1993).

The above discussion suggests that there is still considerable uncertainty regarding to what extent remotely sensed images are (statistically) self-similar and whether self-similarity is a prerequisite to applying fractal techniques. More research is clearly needed in this area. For example, if one accepts that the fractal technique could be used simply as a method to extract textural information, then it may be argued that the structures under consideration do not have to be self-similar. But, do existing computational methods, which operate on the assumption that the object being measured is self-similar/affine, react differently to image textures than to structural self-similarity/affinity in any significant ways? Very little has been written about this issue in the remote sensing literature. Furthermore, if one accepts that statistical self-similarity, when present at all, is exhibited only over limited ranges of scale in real images, then one needs to consider if characterization of image textures using a single (i.e. monofractal) dimension is adequate (discussed in §5.6).

Another issue worth exploring is the use of fractal models to detect edge points in remotely sensed images. Given that breaks in *D* appears to be the norm rather than exception in most real images, it should be possible to extract edge points by identifying breakpoints in estimated *D*. Conceptually, such breakpoints could be considered as the boundaries between homogenous regions with different textural features (Pentland 1984). Research is needed to test such a fractal-based edge detection method using a variety of images and compare it with other existing edge detection algorithms to establish its performance.

5.2 *Method-induced errors*

The utility of *D* as a texture measure depends to a large extent on the reliability of computational methods. A major difficulty in establishing the reliability of various fractal computational methods is that the *D* values computed in different ways are not necessarily related, unless there is a mathematical relationship among the various *D* values. In fact, many studies have shown that different computational methods often yield different results for the same data set (Lam 1990, Clarke and Schweizer 1991, Klinkenberg and Goodchild 1992, De Jong and Burrough 1995, Myint 2003, Sun 2006). The differences among different methods are often so significant that comparisons between computed *D* values obtained using different methods are meaningless. Klinkenberg and Goodchild (1992) have even argued that the variability in computed *D* is more a function of the methods used than it is a reflection of any theoretical inadequacy of the fractal model.

Several factors may be responsible for the observed differences in estimated *D* obtained using different methods (Klinkenberg 1994). First, some of the differences in computed *D* may arise from the fact that fractal computational methods are not all measuring the same fractal quantity. For example, while a stochastic relation is used in the triangular prism method (Clarke 1986) to derive the estimates of *D*, the relation used in those methods based on the walking-dividers approach, such as the isarithm method (Shelberg *et al.* 1983) and the robust fractal estimator (Clarke and Schweizer 1991) discussed above, is a geometric one. Second, part of the differences in computed *D* may result from inappropriately applied methods. For example, the robust fractal estimator (Clarke and Schweizer 1991) can only be applied to self-affine data. Violation of this requirement could lead to erroneous results. Furthermore, even when an appropriate method is chosen, whether the method is executed properly may also affect the results. When working with self-affine data, for example, computation would always return a *D* close to 1 if step sizes exceeded the crossover length. Third, even when an appropriate method is used and properly executed, the details of the estimation process such as the choice of input parameter values may also affect the resultant *D* (discussed below).

Several researchers (Gallant *et al.* 1994, Tate 1998, Lam *et al.* 2002, Sun 2006) have attempted to gauge the direction and magnitude of errors introduced by existing computational methods. Their results show that no single method appears able to produce accurate estimates of *D* over the entire range of *D*. For example, Lam *et al.* (2002) found that the triangular prism method was most accurate for images having higher spatial complexity, for images where generated $D=2.5$ the isarithm returned best results, and the variogram method was a comparatively poor estimator for all surfaces. These results suggest that a particular fractal computational method may be better suited to certain images than others, depending largely on the roughness of the image to be analysed. Practical use of such research findings may be challenged by the fact that relatively little is known about the actual ranges of *D* of different types of remotely sensed images. Furthermore, determination of the degree of 'roughness' of an image would represent a priori knowledge about the textural complexity of the image. Can other existing texture analysis techniques, such as co-occurrence matrices (Haralick *et al.* 1973), wavelets (Mallat 1989), and local variance (Woodcock and Strahler 1987), be used for this purpose? What kind of relationship exists between other measures of texture and the *D*? The existing literature does not seem to provide satisfactory answers to these questions. As such, they constitute a fertile field for future research.

5.3 *Parameter specifications and the computed* D

Implementation of fractal computational methods requires the user to define a certain number of input parameters, such as beginning and ending step sizes, interval spacing (step size), direction of computation, and so forth. The choice of such parameter values is an important issue as these decisions can greatly influence the computed *D*. In the methods discussed above (table 1), the estimate of *D* is derived as some function of the slope of the regression lines and the slope is determined using the least-squares method. This means that the selection of the smallest and largest step sizes and the interval spacing is a critical decision as these parameter values may affect the slope of the regression line and hence the computed

D. However, there are no established guidelines for choosing the beginning or ending step size. Shelberg *et al.* (1982) proposed to use one-half of the average distance between every pair of adjacent points as the smallest step size. Andrle (1992), on the other hand, suggested that the smallest step size be twice the shortest distance between any two points. In practice, the smallest step size is often chosen to be close to the limiting resolution of the datasets used (Clarke and Schweizer 1991). As for the largest step size, several authors have suggested using a reduced largest step size for two reasons. First, use of a smaller largest step size may help minimize the effects of partial steps (Andrle 1992). Second, when working with self-affine profiles, it is critical to ensure that the largest step size remains smaller than the crossover length (Mandelbrot 1985).

It is widely accepted that for statistical reasons, step size should increase as a power of two (i.e. doubling the step size) so that data points on the log–log plot are equally spaced in their independent variable. Doubling the step size will, however, rapidly cover the data and may result in too few data points available for regression analysis if the image being analysed is not sufficiently large. The number of step sizes (or step size increments) is another parameter that needs to be selected with care as this parameter determines the number of data points available for the regression analysis. To obtain reliable results, it is necessary to use a sufficiently large number of step sizes. However, there is no established guideline for choosing an 'appropriate' number of step sizes either. Shelberg *et al.* (1982) suggested that five to eight step size increments be used. It should be noted that the need to use a large number of data points in regression analysis is in conflict with the sampling strategy of doubling the step size, since doubling the step size means that fewer step size increments can be made (Klinkenberg 1994). As such, careful consideration is needed in selecting the beginning and ending step size and the interval spacing.

5.4 *Input data and the computed* D

Several factors related to the remote sensing data used in an analysis may also affect the computed *D*. We outline below some of the factors that require attention in computing the *D* of remotely sensed images.

- To the extent that the image being measured is not strictly self-similar, the spatial resolutions, regions, directions, and sampling process selected as input data may all affect the computed *D*. It may be desirable that in reporting research findings, the researcher gives sufficient details about the input data used. Without such information, comparison of results from different studies would be meaningless.
- Textures of the same land cover feature in different spectral bands are often different in terms of contrast, smoothness, spatial variation, and so forth. Therefore, it is most likely that computed *D* values will vary greatly with the bands chosen. Selecting bands with the 'right' spectral information content will be an important task in fractal analysis of remotely sensed images, if the technique is to be effective in capturing the textural characteristics of the phenomena under consideration.
- The way in which an image is represented, such as the range of pixel values used, may also have an effect on the computed *D* when using certain computational methods. Lam *et al.* (2002), for example, found that the triangular prism method was particularly sensitive to changes in image contrast and recommended that images be normalized before computing *D*.

- The quality of the image used may also affect the estimated *D* as the 'contribution' of noise to the spatial variations in pixel values could be significant. An assessment of image quality using such techniques as the signal-to-noise ratios may be useful (De Jong and Burrough 1995, Emerson *et al.* 1999).

5.5 *Computing local* D *values*

A major contribution of De Jong and Burrough's (1995) work reviewed above is that they demonstrated how to *locally* compute the *D* of real remotely sensed images. This is an important step as most existing methods only yield a lumped *D* value for the entire image. While such global *D* values may be useful for certain purposes, they cannot be used to segment images. Surprisingly few studies have attempted to systematically calculate local *D* values and use such information to classify real images. How to develop efficient algorithms to compute local *D* values from real images and use local *D* values as textural information to improve image classification is an area that holds great potential for future research.

As De Jong and Burrough (1995) have shown, local *D* values can be computed using moving window techniques. As with all other techniques involving kernels, computation of local *D* values must deal with two undesirable effects, i.e. the blurring effect and the boundary effect. In their study, De Jong and Burrough (1995) found that the blurring effects resulted from a 9 by 9 analysis window were visible. Using local windows to compute *D* also means that local *D* values will not be available for certain rows and columns, whose number equals to one half of the local window size used, around the edge of the image being analysed.

A potentially more challenging issue in computing local *D* values is the choice of window size. On one hand, minimization of local window size is required to capture details of local variations in land covers. On the other hand, the regression technique used in the estimation of *D* requires a sufficiently large number of step sizes to be available within an analysis window. This, coupled with the sampling strategy of doubling the step size, means that the window size will be quite large. For example, if the number of step sizes is chosen to be five, this will translate into a local window size of 17 by 17 pixels. Use of large window size may, however, lead to several problems. First, a large window will include more land covers and it can lead to mixed pixel problems. Second, using a large window means that land cover features smaller than the window size will not be identified in classification. Third, using a large window will also lead to loss of more pixels on the edges (i.e. boundary effects). As such, how to choose an 'appropriate' window size for computing local *D* values is an issue that deserves further research.

5.6 *How to better describe image texture using fractal geometry?*

A major finding from the research published to date is that, while fractal dimension appears able to capture certain aspects of the surface properties of remotely sensed images, use of *D* alone cannot sufficiently describe image textures and achieve satisfactory classification results. Several approaches have been suggested to address this problem. Below we briefly discuss three such approaches.

5.6.1 Multi-parameter fractal description of image texture. Most existing studies applying fractal techniques to image texture analysis have concentrated on a single fractal parameter, i.e. the fractal dimension. Certain computational methods, such as the variogram and the Fourier power spectral methods, produce more than just one parameter. Variogram analysis, for example, generates not only the estimate of the slope but estimates for the range and the intercept of a variogram (Chen and Gong 2004). Studies in other fields such as geomorphology have shown that the log–log plot ordinate intercept of a variogram seems to capture certain information that is not captured by D (Klinkenberg 1992). Therefore, it seems desirable to use more fractal parameters to characterize image textures instead of using only D. A disadvantage of this multi-parameter fractal approach is that not all methods can provide parameters other than D.

5.6.2 Multifractal models. All the methods reviewed in this paper are based on a mono-fractal approach, which assumes that the object under consideration can be characterized by a single fractal dimension. Evidence from the geosciences suggests, however, that the various natural processes (geological, geomorphological, ecological, etc) operating at different scales do not have the same influence on the structures in nature (Mark and Aronson 1984, Roy *et al.* 1987, Klinkenberg and Goodchild 1992). As a result, most natural phenomena are characterized by different dominant structures at different scales (Goodchild and Mark 1987, Feder 1988, Mandelbrot 1989, Milne 1991, Meakin 1991). Analysis of real remotely sensed data has also shown that the scaling behaviour of image properties deviates greatly from the ideal mono-fractal dimension assumption (De Cola 1993). This suggests that multifractal models appear to be more suited to characterization of image textures. There is a growing body of literature on the application of multifractal models in image analysis (e.g. Peitgen and Saupe 1988, Arduini *et al.* 1992, De Cola 1993, Fioravanti 1994, Cheng 1999, Parrinello and Vaughan 2002, Posadas *et al.* 2005). A detailed discussion of this literature is beyond the scope of this paper.

5.6.3 Lacunarity and image texture analysis. Fractal dimension is a parameter that measures the geometric complexity of the *shape* of an object. Obviously, shape is not the only property of image texture. Other factors such as the size and distribution of a textural feature and its spatial relations to other features may also play an important part in differentiating one type of texture from another. This means that use of D alone may not be sufficient in characterization of image textures. Mandelbrot (1982) pointed out that different fractal sets may share the same D and yet have strikingly different appearances or textures. This seems to have been borne out in several empirical studies in which the estimated D values of different land cover types were found to be overlapping or even the same (Keller *et al.* 1989, De Jong and Burrough 1995, Myint 2003). Lacunarity analysis is a technique introduced by Mandelbrot (1982) to deal with fractal objects of the same dimension with different textural appearances. Lacunarity is related to the distribution of gap sizes: low lacunarity objects are characterized by similar or same gap sizes and therefore appear homogeneous, whereas high lacunarity objects are heterogeneous (Mandelbrot 1982, Allain and Cloitre 1991, Dong 2000a). Although originally developed for fractal objects, lacunarity analysis has been proposed to be a general technique for the analysis of nonfractal and multifractal patterns (Plotnick *et al.* 1996). Image segmentation using lacunarity or a combination of D and lacunarity seem to have obtained good results (e.g., Keller *et al.* 1989, Dong 2000b). It appears that incorporating lacunarity measures into the classification procedure is another promising approach to enhancing classification results. Readers interested in the methods for computing lacunarity are directed to Mandelbrot (1982), Allain and Cloitre (1991) and Dong (2000b).

6. Conclusions

Fractal geometry appears to provide a useful tool for characterizing textural features in remotely sensed images because most of what we measure in remote sensing—boundaries of land covers, patches of landscapes, rivers and water bodies, tree crowns, etc—is discontinuous, complex, and fragmented. Fractal techniques have been applied to measure the 'roughness' or geometric complexity of land surface features in unclassified and classified images. Quantitative information about local variations in estimated D values has been used as a texture measure to segment remotely sensed images. Fractal techniques have also been used to investigate the scaling behaviour of environmental phenomena and the results from this stream of research may prove valuable for choosing 'optimal' resolutions for studying environmental phenomena at different scales in remote sensing and GIS.

Despite the potential utility of fractal techniques, several methodological and practical measurement problems have been encountered in fractal analysis of remotely sensed images. For example, the computed D is supposed to capture the differences in the characteristics of image textures. However, a host of factors other than image texture, such as the computational method used, the choice of input parameter values, input images, and so forth, may all have an effect on the computed D. As a result, it seems extremely difficult, if possible at all, to determine whether the observed differences in computed D values is a result of true differences in image texture or a result of certain arbitrary decisions made during the estimation process. As such, the question what actually is measured in the computed D remains unanswered.

For D to be a useful parameter, the methods of computing D must be robust, consistent, and have the ability to distinguish visually different textures. Research published to date has shown, however, that significant variations in computed D can be introduced by computational methods. Therefore, the choice of method is an important issue in the computation of D for remotely sensed data. Researchers need to be aware of the comparative performance of different methods proposed in the literature and the biases that are associated with a particular method. Blind use of a method without knowing its applicable D ranges and potential errors may lead to poor or even erroneous results. Given the uncertainty surrounding the nature and extent of method-induced errors, more systematic evaluation of existing computational methods is needed.

A major drawback in using fractal techniques for analysing remotely sensed images is that they can be applied only to single bands[†]. Since real remotely sensed images are generally multispectral ones, it appears desirable to develop what may be called 'multivariate fractal methods.' Such multivariate fractal methods should enable the analysis of all bands together and, therefore, would represent a tremendous improvement to the existing methods in fractal analysis of remotely sensed data.

For the most part, existing research applying fractal techniques to remote sensing problems rests on the assumption that image textures can be described by a single (mono-fractal) dimension. Evidence from remote sensing applications as well as

[†] We thank an anonymous reviewer for bringing this issue to our attention.

other fields of the geosciences suggests that the structures underlying most natural phenomena are most likely multifractals. This implies that fractal analysis of remotely sensed images without checking their dimensionalities may be problematic. More important, further research is needed to determine whether multifractal models could do a better job in characterizing image textures.

The fractal dimension can be thought of as a summary statistic measuring the overall geometric complexity of image textures. Like many summary statistics, the fractal dimension is obtained by 'averaging' local tonal variations and it only captures one aspect of the spatial variations of grey levels in the image. The estimated D of a textural feature, for example, tells us nothing about its actual size or its spatial distribution, nor can we infer its spatial relations to other textural features from its D alone. This may explain why many studies have found that, despite its usefulness, use of D alone is insufficient to accurately describe image textures and achieve satisfactory classification results. It appears that the utility of D may be explored to a fuller extent when it is used in conjunction with other texture measures and perhaps spectral classification approaches as well.

Acknowledgements
We would like to thank three anonymous reviewers for their very helpful comments on an earlier draft of this paper.

References

ALLAIN, C. and CLOITRE, M., 1991, Characterizing the lacunarity of random and determined fractal set. *Physics Review A*, **44**, pp. 3552–3558.

ANDRLE, R., 1992, Estimating fractal dimension with the divider method in geomorphology. *Geomorphology*, **5**, pp. 131–141.

ARDUINI, F., FIORAVANTI, S. and GIUSTO, D.D., 1992, On computing multifractality for texture discriminiation. In *Proceedings of EUSIPCO-92*, 24–27 August 1992, Brussels, Belgium, J. Vandewelle and R. Boite (Eds) (Brussels: Elsevier Science), pp. 1457–1461.

ARMSTRONG, A., 1986, On the fractal dimensions of some transient soil properties. *Journal of Soil Science*, **37**, pp. 641–652.

BARNSLEY, M.F., 1989, Iterated function systems. In *Chaos and Fractals: Mathematics behind the Computer*, R.L. Devaney and L. Keen (Eds), pp. 127–144 (Providence, RI: American Mathematical Society).

BATTY, M. and LONGLEY, P.A., 1986, The fractal simulation of urban structure. *Environment and Planning A*, **18**, pp. 1143–1179.

BELLOULATA, K. and KONRAD, J., 2002, Fractal image compression with region-based functionality. *IEEE Transactions on Image Processing*, **11**, pp. 351–362.

BLACHER, S., BROUERS, F. and VAN DYCK, R., 1993, On the use of fractal concepts in image analysis. *Physica A*, **197**, pp. 516–527.

BROWN, S.R., 1995, Measuring the dimension of self-affine fractals: examples of rough surfaces. In *Fractals in the Earth Sciences*, C.C. Barton and P.R. La Pointe (Eds), pp. 77–87 (New York: Plenum Press).

BURROUGH, P.A., 1981, Fractal dimensions of landscapes and other environmental data. *Nature*, **294**, pp. 240–242.

BURROUGH, P.A., 1993, Fractals and geostatistical methods in landscape studies. In *Fractals in Geography*, N.S.-N. Lam and L. De Cola (Eds), pp. 87–121 (New Jersey: Prentice Hall).

CALVET, L. and FISHER, A., 2002, Multifractality in asset returns: Theory and practice. *Reviews of Economics and Statistics*, **84**, pp. 381–406.

CARR, J. and BENZER, W., 1991, On the practice of estimating fractal dimension. *Mathematical Geology*, **23**, pp. 945–958.

CHAUDHURI, B.B., SARKAR, N. and KUNDU, P., 1993, Improved fractal geometry based texture segmentation technique. *IEEE Proceedings E*, **140**, pp. 233–241.

CHEN, Q. and GONG, P., 2004, Automatic variogram parameter extraction for textural classification of IKONOS imagery. *IEEE Transactions on Geoscience and Remote Sensing*, **42**, pp. 1106–1115.

CHEN, C.C., DAPONTE, J.S. and FOX, M.D., 1989, Fractal feature analysis and classification in medical imaging. *IEEE Transactions on Medical Imaging*, **6**, pp. 133–142.

CHENG, Q., 1999, Multifractality and spatial statistics. *Computers and Geosciences*, **25**, pp. 949–961.

CLARKE, K.C., 1986, Computation of the fractal dimension of topographic surfaces using the triangular prism surface area method. *Computers and Geosciences*, **12**, pp. 713–722.

CLARKE, K.C. and SCHWEIZER, D.M., 1991, Measuring the fractal dimension of natural surfaces using a robust fractal estimator. *Cartography and Geographic Information Systems*, **18**, pp. 37–47.

CLIFF, A.D. and ORD, J.K., 1973, *Spatial Autocorrelation* (London: Pion Limited).

DE COLA, L., 1989, Fractal Analysis of a classified Landsat scene. *Photogrammetric Engineering and Remote Sensing*, **55**, pp. 601–610.

DE COLA, L., 1993, Multifractals in image processing and process imaging. In *Fractals in Geography*, N.S.-N. Lam and L. De Cola (Eds), pp. 282–304 (New Jersey: Prentice Hall).

DE JONG, S.M., 1993, An application of spatial filtering techniques for land cover mapping using TM images. *Geocarto International*, **8**, pp. 43–49.

DE JONG, S.M. and BURROUGH, P.A., 1995, A fractal approach to the classification of Mediterranean vegetation types in remotely sensed images. *Photogrammetric Engineering and Remote Sensing*, **61**, pp. 1041–1053.

DENNIS, T.J. and DESSIPRIS, N.G., 1989, Fractal modeling in image texture analysis. *IEEE Proceedings*, **136**, pp. 227–235.

DEVANEY, R.L. and KEEN, L., 1989, *Chaos and Fractals: Mathematics Behind the Computer* (Providence, RI: American Mathematical Society).

DONG, P.L., 2000a, Lacunarity for spatial heterogeneity measurement in GIS. *Geographic Information Sciences*, **6**, pp. 20–26.

DONG, P.L., 2000b, Test of a new lacunarity estimation method for image texture analysis. *International Journal of Remote Sensing*, **17**, pp. 3369–3373.

DYSON, F., 1978, Characterizing irregularity. *Science*, **200**, pp. 677–678.

EMERSON, C.W., LAM, N.S.-N. and QUATTROCHI, D.A., 1999, Multiscale fractal analysis of image texture and pattern. *Photogrammetric Engineering and Remote Sensing*, **65**, pp. 51–61.

EMERSON, C.W., QUATTROCHI, D.A. and LAM, N.S.-N., 2004, Spatial metadata for remote sensing imagery. Available online at: www.esto.nasa.gov/conferences/estc2004/papers/b8p2.pdf (accessed 10 May 2005).

FEDER, J., 1988, *Fractals* (New York: Plenum Press).

FIORAVANTI, S., 1994, Multifractals: theory and application to image texture recognition. In *Fractals in Geoscience and Remote Sensing, Proceedings of A Joint JRC/EARSeL Expert Meeting*, pp. 152–175 (Luxemburg: European Commission).

FOURNIER, A., FUSSELL, D. and CARPENTER, L., 1982, Computer rendering of stochastic models. *Communications of the ACM*, **25**, pp. 371–384.

FOX, C. and HAYES, D.E., 1985, Quantitative methods for analyzing the roughness of the seafloor. *Reviews of Geophysics*, **23**, pp. 1–48.

GALLANT, J.C., MOORE, I.D., HUTCHINSON, M.F. and GESSLER, P., 1994, Estimating fractal dimension of profiles: A comparison of methods. *Mathematical Geology*, **26**, pp. 455–481.

GAO, J. and XIA, Z.G., 1996, Fractals in physical geography. *Progress in Physical Geography*, **20**, pp. 178–191.

GERMAIN, M., BENIE, G.B., BOUCHER, J.M., FOUCHER, S., FUNG, K. and GOITA, K., 2003, Contribution of the fractal dimension to multiscale adaptive filtering of SAR imagery. *IEEE Transactions on Geosciences and Remote Sensing*, **41**, pp. 1765–1772.

GHAZEL, M., FREEMAN, G.H. and VRSCAY, E.R., 2003, Fractal image denoising. *IEEE Transactions on Image Processing*, **12**, pp. 1560–1578.

GONG, P. and HOWARTH, P.J., 1990, The use of structural information for improving land-cover classification accuracies at the rural-urban fringe. *Photogrammetric Engineering and Remote Sensing*, **56**, pp. 67–73.

GONG, P., MARCEAU, D.J. and HOWARTH, P.J., 1992, A comparison of spatial feature extraction algorithms for land-use classification with SPOT HRV data. *Remote Sensing of Environment*, **40**, pp. 137–151.

GOODCHILD, M.F., 1980, Fractals and the accuracy of geographical measures. *Mathematical Geology*, **12**, pp. 85–98.

GOODCHILD, M.F. and MARK, D.M., 1987, The fractal nature of geographic phenomena. *Annals of the Association of American Geographers*, **77**, pp. 265–278.

GREEN, T.R. and ERSKINE, R.H., 2004, Measurement, scaling, and topographic analyses of spatial crop yield and soil water content. *Hydrological Processes*, **18**, pp. 1447–1465.

HARALICK, R.M., SHANMUGAN, K. and DINSTEIN, I., 1973, Texture features for image classification. *IEEE Transactions on Systems, Man, and Cybernetics*, SMC–3, pp. 610–621.

HE, H.S., VENTURA, S.J. and MLADENOFF, D.J., 2002, Effects of spatial aggregation approaches on classified satellite imagery. *International Journal of Geographical Information Science*, **16**, pp. 93–109.

JAGGI, S., QUATTROCHI, D.A. and LAM, N.S.-N., 1993, Implementation and operation of three fractal measurement algorithms for analysis of remote-sensing data. *Computer and Geosciences*, **19**, pp. 745–767.

JONES, J., THOMAS, R. and EARWICKER, P., 1989, Fractal properties of computer-generated and natural geophysical data. *Computers and Geosciences*, **15**, pp. 227–235.

KELLER, J.M., CROWNOVER, R.M. and CHEN, R.Y., 1987, Characteristics of natural scenes related to the fractal dimension. *IEEE Transactions on Pattern Analysis and Machine Intelligence*, **9**, pp. 621–627.

KELLER, J.M., CHEN, S. and CROWNOVER, R.M., 1989, Texture description and segmentation through fractal geometry. *Computer Vision, Graphics, and Image Processing*, **45**, pp. 150–166.

KENNEDY, S.K. and LIN, W., 1986, FRACT—A Fortran subroutine to calculate the variables necessary to determine the fractal dimension of closed forms. *Computers and Geosciences*, **12**, pp. 705–712.

KLINKENBERG, B., 1992, Fractal and morphometric measures: Is there a relationship? *Geomorphology*, **5**, pp. 5–20.

KLINKENBERG, B., 1994, A review of methods used to determine the fractal dimension of linear features. *Mathematical Geology*, **26**, pp. 23–46.

KLINKENBERG, B. and GOODCHILD, M.F., 1992, The fractal properties of topography: A comparison of methods. *Earth Surface Processes and Landforms*, **17**, pp. 217–234.

LAGRO JR, J., 1991, Assessing patch shape in landscape mosaics. *Photogrammetric Engineering and Remote Sensing*, **57**, pp. 285–293.

LAM, N.S.-N., 1990, Description and measurement of Landsat TM images using fractals. *Photogrammetric Engineering and Remote Sensing*, **56**, pp. 187–195.

LAM, N.S.-N. and DE COLA, L., 1993a, *Fractals in Geography* New Jersey: Prentice Hall).

LAM, N.S.-N. and DE COLA, L., 1993b, Fractal measurement. In *Fractals in Geography*, N.S.-N. Lam and L. De Cola (Eds), pp. 23–55 (New Jersey: Prentice Hall).

LAM, N.S.-N., QIU, H.L., QUATTROCHI, D.A. and EMERSON, C.W., 2002, An evaluation of fractal methods for characterizing image complexity. *Cartography and Geographic Information Science*, **29**, pp. 25–35.

LEE, W.L., CHEN, Y.C. and HSIEH, K.S., 2003, Ultrasonic liver tissues classification by fractal feature vector based on M-band wavelet transform. *IEEE Transactions on Medical Imaging*, **22**, pp. 382–392.

LIANG, S., 2004, *Quantitative Remote Sensing of Land Surfaces* (New York: John Wiley & Sons).

LOEHLE, C., 1983, The fractal dimension and ecology. *Speculations in Science and Technology*, **6**, pp. 131–142.

LORIMER, N.D., HAIGHT, R.G. and LEARY, R.A., 1994, *The Fractal Forest: Fractal Geometry and Applications in Forest Science* (USDA: General Technical Report NC–170).

LOVEJOY, S., 1982, Area-perimeter relation for rain and cloud areas. *Science*, **216**, pp. 185–187.

LOVEJOY, S. and SCHERTZER, D., 1985, Generalized scale invariance in the atmosphere and fractal models of rain. *Water Resources Research*, **21**, pp. 1233–1250.

LOVEJOY, S. and SCHERTZER, D., 1990, Fractals, rain drops, and resolution dependence of rain measurements. *Journal of Applied Meteorology*, **29**, pp. 1167–1170.

LU, S.Z. and HELLAWELL, A., 1995, Using fractal analysis to describe irregular microstructures. *Journal of Materials*, **47**, pp. 14–16.

MAITRE, H. and PINCIROLI, M., 1999, Fractal characterization of a hydrological basin using SAR satellite images. *IEEE Transactions on Geosciences and Remote Sensing*, **37**, pp. 175–181.

MALLAT, S.G., 1989, A theory for multi-resolution signal decomposition: The wavelet representation. *IEEE Transactions on Pattern Analysis and Machine Intelligence*, **11**, pp. 674–693.

MANDELBROT, B.B., 1967, How long is the coast of Britain? Statistical self-similarity and fractional dimension. *Science*, **156**, pp. 636–638.

MANDELBROT, B.B., 1977, *Fractals: Form, Chance and Dimension* (San Francisco, CA: W.H. Freeman and Company).

MANDELBROT, B.B., 1982, *The Fractal Geometry of Nature* (New York: W.H. Freeman and Company).

MANDELBROT, B.B., 1985, Self-affine fractals and the fractal dimension. *Physica Scripta*, **32**, pp. 257–260.

MANDELBROT, B.B., 1989, Multifractal measures, especially for the geophysicists. *Pageoph*, **131**, pp. 5–42.

MANDELBROT, B.B. and HUDSON, R.L., 2004, *The (mis)Behavior of Markets: A fractal view of risk, ruin, and reward* (New York: Basic Books).

MARK, D.M. and ARONSON, P.B., 1984, Scale-dependent fractal dimensions of topographic surfaces: An empirical investigation with application in geomorphology and computer Mapping. *Mathematical Geology*, **16**, pp. 671–683.

MEAKIN, P., 1991, Fractal aggregates in geophysics. *Reviews of Geophysics*, **29**, pp. 317–354.

MILNE, B.T., 1991, Lessons from applying fractal models to landscape patterns. In *Quantitative Methods in Landscape Ecology*, M.G. Turner and R.H. Gardern (Eds), pp. 199–235 (New York: Springer Verlag).

MYINT, S.W., 2003, Fractal approaches in texture analysis and classification of remotely sensed data: Comparisons with spatial autocorrelation techniques and simple descriptive statistics. *International Journal of Remote Sensing*, **24**, pp. 1925–1947.

NORMANT, F. and TRICOT, C., 1993, Fractal simplification of lines using convex hulls. *Geographical Analysis*, **25**, pp. 118–129.

ORFORD, J.D. and WHALLEY, W.B., 1983, The use of the fractal dimension to quantify the morphology of irregular-shaped particles. *Sedimentology*, **30**, pp. 655–668.

PACHEPSKY, Y.A., RITCHIE, J.C. and GIMENEZ, D., 1997, Fractal modeling of airborne laser altimetry data. *Remote Sensing of Environment*, **61**, pp. 150–161.

PARRINELLO, T. and VAUGHAN, R.A., 2002, Multifractal analysis and feature extraction in satellite imagery. *International Journal of Remote Sensing*, **23**, pp. 1799–1825.

PEITGEN, H.O. and RICHTER, P.H., 1986, *The Beauty of Fractals* (New York: Springer Verlag).

PEITGEN, H.O. and SAUPE, D., 1988, *The Science of Fractal Images* (New York: Springer Verlag).

PELEG, S., NAOR, J., HARTLEY, R. and AVNIR, D., 1984, Multiple resolution texture analysis and classification. *IEEE Transactions on Pattern Analysis and Machine Intelligence*, **6**, pp. 518–528.

PENTLAND, A.P., 1984, Fractal-based descriptions of natural scenes. *IEEE Transactions on Pattern Analysis and Machine Intelligence*, **6**, pp. 661–674.

PIECH, M.A. and PIECH, K.R., 1990, Fingerprints and fractal terrain. *Mathematical Geology*, **22**, pp. 457–485.

PLOTNICK, R.E., GARDNER, R.H., HARGROVE, W.W., PRESTEGARRD, K. and PERLMUTTER, M., 1996, Lacunarity analysis: A general technique for the analysis of spatial patterns. *Physical Review E*, **53**, pp. 5461–5468.

POSADAS, A.N.D., QUIROZ, R., ZOROGASTUA, P.E. and LEON-VELARDE, C., 2005, Multifractal characterization of the spatial distribution of ulexite in a Bolivian salt flat. *International Journal of Remote Sensing*, **26**, pp. 615–627.

PRATT, W.K., FAUGERAS, O.D. and GAGALOWICZ, A., 1978, Visual discrimination of stochastic texture fields. *IEEE Transactions on Systems, Man and Cybernetics*, SMC–8, pp. 796–804.

QIU, H., LAM, N.S.-N., QUATTOCHI, D.A. and GAMON, J.A., 1999, Fractal characterization of hyperspectral imagery. *Photogrammetric Engineering and Remote Sensing*, **65**, pp. 63–71.

READ, J.M. and LAM, N.S.-N., 2002, Spatial methods for characterizing land cover and detecting land-cover changes for the tropics. *International Journal of Remote Sensing*, **23**, pp. 2457–2474.

RICHARDSON, L.F., 1961, The problem of contiguity: An appendix to "Statistics of Deadly Quarrels." *General Systems Yearbook*, **6**, pp. 139–187.

RICOTTA, C. and AVENA, G.C., 1998, Fractal modeling of the remotely sensed two-dimensional net primary production pattern with annual cumulative AVHRR NDVI data. *International Journal of Remote Sensing*, **19**, pp. 2413–2418.

RICOTTA, C., AVENA, G.C., OLSEN, E.R., RAMSEY, R.D. and WINN, D.S., 1998, Monitoring the landscape stability of Mediterranean vegetation in relation to fire with a fractal algorithm. *International Journal of Remote Sensing*, **19**, pp. 871–881.

ROY, A.G., GRAVEL, G. and GAUTHIER, C., 1987, Measuring the dimension of surfaces: A review and appraisal of different methods. *Proceedings of the Eighth International Symposium on Computer-Assisted Cartography* (Auto–Carto **8**), pp. 68–77.

SARKAR, N. and CHAUDHURI, B.B., 1992, An efficient approach to estimate fractal dimension of textural images. *Pattern Recognition*, **25**, pp. 1035–1041.

SHELBERG, M.C., MOELLERING, H. and LAM, N.S.-N., 1982, Measuring the fractal dimension of empirical cartographic curves. *Proceedings of the Fifth International Symposium on Computer-Assisted Cartography* (Auto-Carto **5**), pp. 481–490.

SHELBERG, M.C., LAM, N.S.-N. and MOELLERING, H., 1983, Measuring the fractal dimension of surfaces. *Proceedings of the Sixth International Symposium on Computer-Assisted Cartography* (Auto–Carto **6**), pp. 319–328.

SUN, W., 2005, Three new implementations of the triangular prism method for computing the fractal dimension of remote sensing images. *Photogrammetric Engineering and Remote Sensing*, **72**, pp. 373–382.

SUN, W., KOLAPPAL, A.Z. and GONG, P., 2006, Two computational methods for detecting anisotropy in image texture. *Geographic Information Science* (forthcoming).

TATE, N.J., 1998, Estimating the fractal dimension of synthetic topographic surfaces. *Computers and Geosciences*, **24**, pp. 325–334.

TSO, B. and MATHER, P.M., 2001, *Classification Methods for Remotely Sensed Data* (London: Taylor and Francis).

TURCOTTE, D.L., 1992, *Fractals and Chaos in Geology and Geophysics* (Cambridge: Cambridge University Press).

VOSS, R., 1988, Fractals in nature: From characterization to simulation. In *The Science of Fractal Images*, H.O. Peitgen and D. Saupe (Eds), pp. 21–70 (New York: Springer Verlag).

WANG, L. and HE, D.C., 1990, A new statistical approach for texture analysis. *Photogrammetric Engineering and Remote Sensing*, **56**, pp. 61–66.

WENG, Q., 2003, Fractal analysis of satellite-detected urban heat island effect. *Photogrammetric Engineering and Remote Sensing*, **69**, pp. 555–566.

WESZKA, J., DYER, C.R. and ROSENFELD, A., 1976, A comparative study of texture measures for terrain classification. *IEEE Transactions on Systems, Man, and Cybernetics*, **SMC-6**, pp. 269–285.

WIENS, J.A., 1989, Spatial scaling in ecology. *Functional Ecology*, **3**, pp. 385–397.

WOODCOCK, C.E. and STRAHLER, A.H., 1987, The factor of scale in remote sensing. *Remote Sensing of Environment*, **21**, pp. 311–332.

WU, C.M., CHEN, Y.C. and HSIEH, K.S., 1992, Texture features for classification of ultrasonic liver images. *IEEE Transactions on Medical Imaging*, **11**, pp. 141–152.